

Preparation of DSA@MNPs and application as heterogeneous and recyclable nanocatalyst for oxidation of sulfides and oxidative coupling of thiols

Arash Ghorbani-Choghamarani¹ ·
Hossein Rabiei¹ · Bahman Tahmasbi¹ ·
Banoo Ghasemi¹ · Farideh Mardi¹

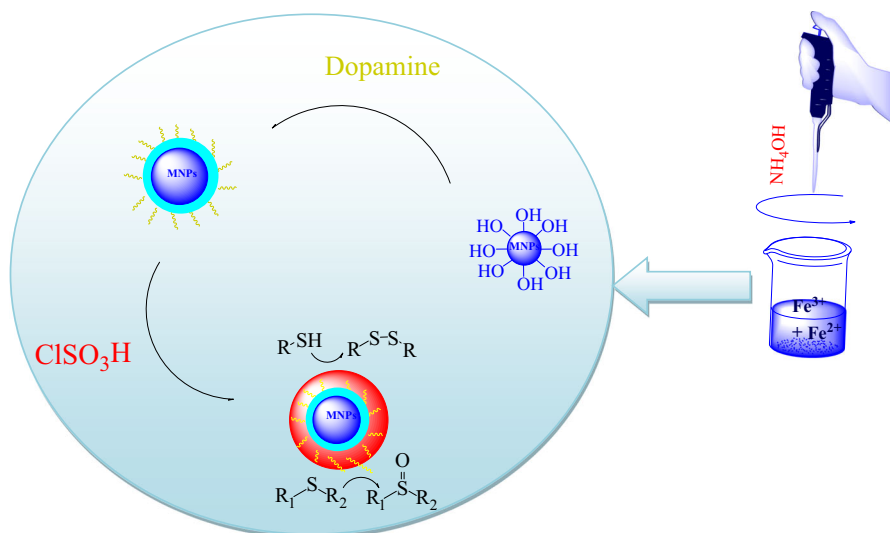
Received: 2 July 2015 / Accepted: 16 December 2015
© Springer Science+Business Media Dordrecht 2016

Abstract Dopamine sulfamic acid-functionalized magnetic Fe₃O₄ nanoparticles (DSA@MNPs) were prepared by a very simple and inexpensive procedure using commercial materials and characterized by X-ray diffraction (XRD) analysis, thermogravimetric analysis (TGA), Fourier-transform infrared (FT-IR) spectroscopy, scanning electron microscopy (SEM), transmission electron microscopy (TEM), and vibrating-sample magnetometry (VSM) techniques. They were employed as an efficient and recoverable catalyst in oxidation of sulfides to sulfoxides and oxidative coupling of thiols to disulfides using hydrogen peroxide as green oxidant at room temperature. This is the first report of application of DSA@MNPs in organic reactions. The supported magnetic nanoparticles could be easily recovered using an appropriate external magnet, minimizing catalyst loss during separation, and reused for several times without any loss of catalytic activity. Also, the amount of sulfamic acid function in the DSA@MNPs was calculated from ion-exchange pH analysis and back titration.

✉ Arash Ghorbani-Choghamarani
a.ghorbani@mail.ilam.ac.ir; arashghch58@yahoo.com

¹ Department of Chemistry, Ilam University, P.O. Box 69315516, Ilam, Iran

Graphical abstract



Keywords Hydrogen peroxide · Dopamine · Magnetic nanoparticles · Sulfoxide · Disulfide

Introduction

Nanomaterials have provoked wide interest because of their unique properties, being used in biology [1], physics [2], and chemistry [3]. In recent decades, nanotechnology has pushed forward synthesis of functional magnetic nanoparticles (MNPs) for use as heterogeneous catalysts [4]. In general, catalysts can be divided into two groups: homogeneous and heterogeneous systems [5]. In spite of the various benefits of homogeneous catalysts, heterogeneous catalysts are widely applied because of their facile recyclability [6].

Surface-functionalized iron oxide magnetic nanoparticles (MNPs), which have been widely used in biotechnology [7] and analysis [8], offer incomparable advantages over traditional catalysts because of their high activity, magnetic recyclability, and reusability [9].

Mineral liquid acids (such as HF and H_2SO_4) and Lewis acids (such as AlCl_3 and BF_3) are still used as catalysts for organic reactions such as alkylation [10], acylation [11], oxidation, and isomerization [12]. In recent years, solid acid catalysts have served as important functional materials in chemical reactions because of their superacidity, high activity at low temperatures, and nontoxicity [13]. However, preparation of various heterogeneous supports used previously, such as MCM-41 [3], SBA-15 [14], or various nanoparticles such as TiO_2 NPs [15], requires high calcination temperatures or long time and tedious conditions. Other previously reported materials such as heteropolyacids [16], carbon nanotubes [17], ionic liquids [18], or various polymers [19] are more

expensive. However, Fe_3O_4 MNPs can be prepared in water in short time using commercial materials such as $\text{FeCl}_3 \cdot 4\text{H}_2\text{O}$ and $\text{FeCl}_2 \cdot 4\text{H}_2\text{O}$. In addition, one of the attractive features of magnetic nanoparticles is the rapid (within 10 s) and efficient (100 %) separation of the catalyst using an appropriate external magnet, minimizing catalyst loss during separation; this effect is not observed in the case of other supported catalysts, especially nanocatalysts, because they cannot be easily recovered and recycled by filtration [20, 21].

This is the first report of preparation of DSA@MNPs for application as a solid acid catalyst for oxidation of organosulfur compounds with importance in synthetic chemistry, biochemistry, and industrial chemistry. In numerous studies reported in literature, hydrogen peroxide (with only H_2O as byproduct) was applied as an inexpensive and environmentally friendly oxidant for this conversion [22–25]. The whole process for preparation of DSA@MNPs took less than a day, without tedious conditions. More importantly, dopamine and chlorosulfuric acid are commercially available and not expensive.

Experimental

Materials

All reagents and solvents used in this work were purchased from Sigma-Aldrich, Fluka or Merck chemical companies and used without further purification. The particle size and morphology were investigated by scanning electron microscopy (SEM, JEOL JEM-2010) at accelerating voltage of 200 kV. Thermogravimetric analysis (TGA) curves were recorded using a PL-STA 1500 device manufactured by Thermal Sciences. Particle size and morphology were investigated using transmission electron microscopy (TEM, Zeiss-EM10C) at accelerating voltage of 80 kV. VSM measurements were performed using a MDKFD vibrating-sample magnetometer. Magnetization measurements were carried out in an external field of up to 15 kOe at several temperatures. IR spectra were recorded from KBr pellets on a Bruker VRTX 70 model FT-IR spectrophotometer.

Preparation of magnetic Fe_3O_4 nanoparticles (MNPs)

Fe_3O_4 nanoparticles were prepared by chemical coprecipitation of Fe^{3+} and Fe^{2+} ions at molar ratio of 2:1. A mixture of $\text{FeCl}_3 \cdot 6\text{H}_2\text{O}$ (2.35 g, 8.7 mmol) and $\text{FeCl}_2 \cdot 4\text{H}_2\text{O}$ (0.86 g, 4.3 mmol) was dissolved in 40 mL deionized water under nitrogen atmosphere with rapid mechanical stirring. Then, 10 mL NH_4OH solution was added, and black precipitate formed immediately. The black magnetite nanoparticles were isolated by magnetic decantation, washed several times with deionized water, and further washed with ethanol and dried in vacuum [26].

Preparation of MNPs coated by 4-(2-aminoethyl)benzene-1,2-diol (dopamine)

The resulting MNP powder (2 g) was dispersed in 25 mL water using an ultrasonic bath for 30 min. Subsequently, 4-(2-aminoethyl)benzene-1,2-diol (dopamine) (2 g)

was added. The solution was stirred mechanically for 24 h at room temperature. Then, dopamine-functionalized magnetic Fe_3O_4 nanoparticles were separated using an external magnet, washed with deionized water and *n*-hexane three times, and dried at room temperature under vacuum.

Preparation of sulfamic acid-functionalized magnetic Fe_3O_4 nanoparticles

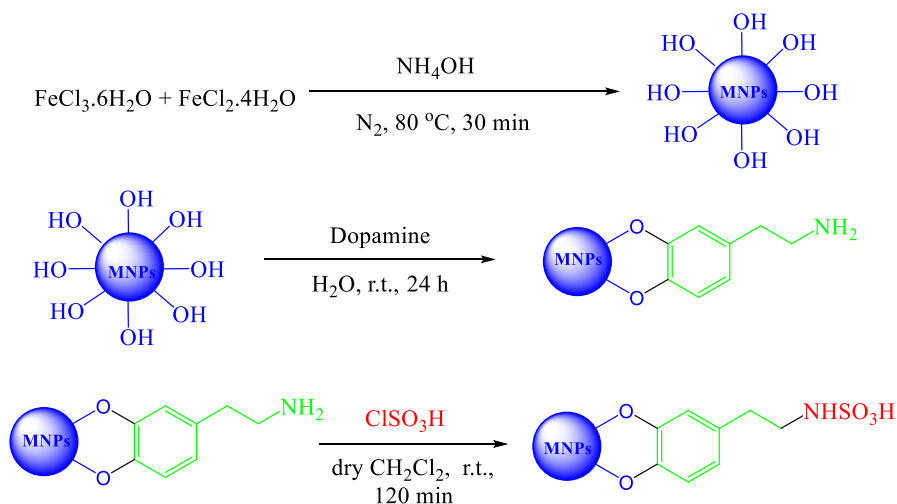
The MNPs–dopamine (0.9 g) was dispersed in *n*-hexane (10 mL) using an ultrasonic bath for 20 min. Then, chlorosulfuric acid (0.2 mL) was added dropwise over a period of 20 min, and the mixture was stirred for 2 h at room temperature. Functionalized MNPs were separated by magnetic decantation, washed four times with dry CH_2Cl_2 and two times with EtOH, and dried at room temperature (Scheme 1).

General procedure for oxidation of sulfides to sulfoxides

Dopamine sulfamic acid-functionalized magnetic Fe_3O_4 nanoparticles (DSA@MNPs) (0.02 g) were added to solution of sulfide (1 mmol) and 33 % H_2O_2 (0.5 mL) in ethanol (10 mL), the mixture was stirred at room temperature for the specified time, and the progress of the reaction was monitored by thin-layer chromatography (TLC). After completion of the reaction, the catalyst was separated using an external magnet. The product was extracted with CH_2Cl_2 , washed with water (5 mL), and dried under vacuum at room temperature.

General procedure for oxidative coupling of thiols

Dopamine sulfamic acid-functionalized magnetic Fe_3O_4 nanoparticles (DSA@MNPs) (0.004 g) were added to solution of thiol (1 mmol) and H_2O_2



Scheme 1 Synthesis of DSA@MNPs

33 % (0.5 mL) in ethanol (10 mL). The reaction mixture was stirred at room temperature, and the progress of the reaction was monitored by TLC. After completion of the reaction, the catalyst was separated using an external magnet, and the product was extracted with CH_2Cl_2 and dried over anhydrous Na_2SO_4 . Finally, the solvent was removed by simple evaporation to give the corresponding pure disulfides.

Selected spectral data

1-(Propylsulfinyl)propane (Table 5, entry 2) ^1H NMR (400 MHz, CDCl_3): δ = 1.13 (t, J = 6 Hz, 6H), 1.86–1.95 (m, 4H), 2.64–2.97 (m, 4H) ppm.

2-((Methylsulfinyl)methyl)furan (Table 5, entry 3) ^1H NMR (400 MHz, CDCl_3): δ = 2.57 (s, 3H), 4.05 (d, J = 14 Hz, 1H), 4.16 (d, J = 14 Hz, 1H), 6.44 (d, J = 3.2 Hz, 1H), 7.17–7.56 (m, 2H) ppm.

((Methylsulfinyl)methyl)benzene (**2c**, Table 5, entry 4) ^1H NMR (250 MHz, CDCl_3): δ = 2.46 (s, 3H), 3.94 (d, J = 17 Hz, 1H), 4.13 (d, J = 17 Hz, 1H), 7.34 (s, 5H) ppm.

Tetrahydrothiophene 1-oxide (Table 5, entry 6) ^1H NMR (400 MHz, CDCl_3): δ = 2.27 (t, J = 7.6 Hz, 2H), 3.06 (t, J = 7.6 Hz, 2H) ppm.

Methyl 3-(methylsulfinyl)propanoate (Table 5, entry 7) ^1H NMR (250 MHz, CDCl_3): δ = 2.85 (t, J = 7.6 Hz, 2H), 2.95 (s, 3H), 3.36 (t, J = 7.5 Hz, 2H), 3.75 (s, 3H) ppm.

*1,2-Di-*p*-tolylidisulfane* (Table 6, entry 2) ^1H NMR (400 MHz, CDCl_3): δ = 2.35 (s, 6H), 7.14 (d, J = 7.9 Hz, 4H), 7.41 (d, J = 7.9 Hz, 4H) ppm.

1,2-Bis(benzo[d]thiazol-2-yl)disulfane (Table 6, entry 4) ^1H NMR (400 MHz, CDCl_3): δ = 7.38 (t, J = 3.2 Hz, 2H), 7.46 (t, J = 3.2 Hz, 2H), 7.78 (d, J = 3.2 Hz, 2H), 7.96 (d, J = 3.2 Hz, 2H) ppm.

1,2-Bis(4,6-dimethylpyrimidin-2-yl)disulfane (Table 6, entry 5) ^1H NMR (400 MHz, CDCl_3): δ = 2.39 (s, 12H), 6.76 (s, 2H) ppm.

2,2'-Disulfanedioldiethanol (Table 6, entry 7) ^1H NMR (400 MHz, CDCl_3): δ = 2.58 (br, 2H), 2.89 (t, J = 5.6 Hz, 4H), 3.91 (t, J = 5.6 Hz, 4H) ppm.

1,2-Di(naphthalen-2-yl)disulfane (Table 6, entry 9) ^1H NMR (400 MHz, CDCl_3): δ = 7.47 (m, 4H), 7.65 (m, 2H), 7.76 (m, 2H), 7.81 (m, 4H), 8.11 (s, 2H) ppm.

1,2-Bis(4-bromophenyl)disulfane (Table 6, entry 10) ^1H NMR (400 MHz, CDCl_3): δ = 7.35 (d, J = 8.2 Hz, 4H), 7.43 (t, J = 8.2 Hz, 4H) ppm.

Results and discussion

Characterization of DSA@MNPs as solid acid catalyst

The morphology and size of the DSA@MNPs were investigated by scanning electron microscopy (SEM, Fig. 1) and transmission electron microscopy (TEM, Fig. 2). It can be seen that most of the particles are quasispherical with homogeneous average diameter of about 15–25 nm.

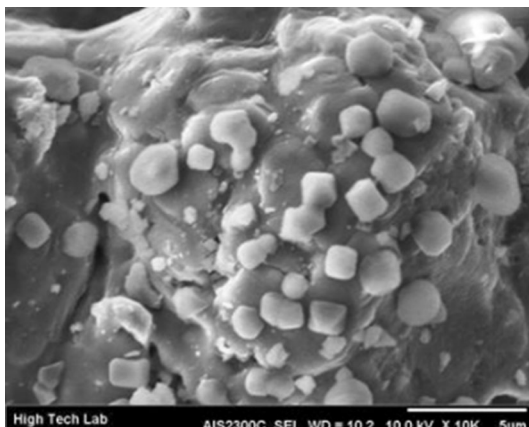
Formation of magnetite crystal phase in the DSA@MNP aggregate powder was identified from the X-ray diffraction pattern. Figure 3 shows the XRD patterns for Fe_3O_4 MNPs and DSA@MNPs. As shown in Fig. 3, seven characteristic peaks ($2\theta = 21.32^\circ, 35.27^\circ, 41.59^\circ, 50.68^\circ, 63.17^\circ, 67.55^\circ$, and 74.51°) were observed, in good agreement with the standard Fe_3O_4 XRD spectrum. This analysis shows that the surface modification of the Fe_3O_4 nanoparticles did not lead to phase changes.

The average diameter of the DSA@MNPs was calculated to be 24 ± 1.6 nm from the XRD results using Scherrer's equation: $D = k\lambda/\beta\cos\theta$, as confirmed by TEM (Fig. 2) and SEM (Fig. 1) techniques.

Figure 4 shows Fourier-transform infrared (FT-IR) spectra of (a) magnetic Fe_3O_4 nanoparticles, (b) MNPs–dopamine, and (c) DSA@MNPs. The FT-IR spectrum for Fe_3O_4 alone shows stretching vibration at $3200\text{--}3400\text{ cm}^{-1}$ which incorporates the contributions from both symmetrical and asymmetrical modes of O–H bonds attached to the surface of magnetic nanoparticles. The strong absorption near 573 cm^{-1} is characteristic of Fe–O bond stretching vibration. In curve (b), which is the spectrum of dopamine-functionalized MNPs, a peak near 1625 cm^{-1} is assigned to N–H bending vibrations and peaks near 1425 cm^{-1} are assigned to C–N stretching vibrations. The reaction of terminal NH_2 groups with ClSO_3H was characterized by a $1000\text{--}1300\text{ cm}^{-1}$ band which can indicate SO_3H groups.

Also, in the FT-IR spectrum of MNPs–dopamine, the presence of anchored dopamine group is confirmed by N–H stretching vibration modes appearing at about 3400 cm^{-1} . Reaction of MNPs–dopamine with chlorosulfuric acid produced

Fig. 1 SEM image of DSA@MNPs



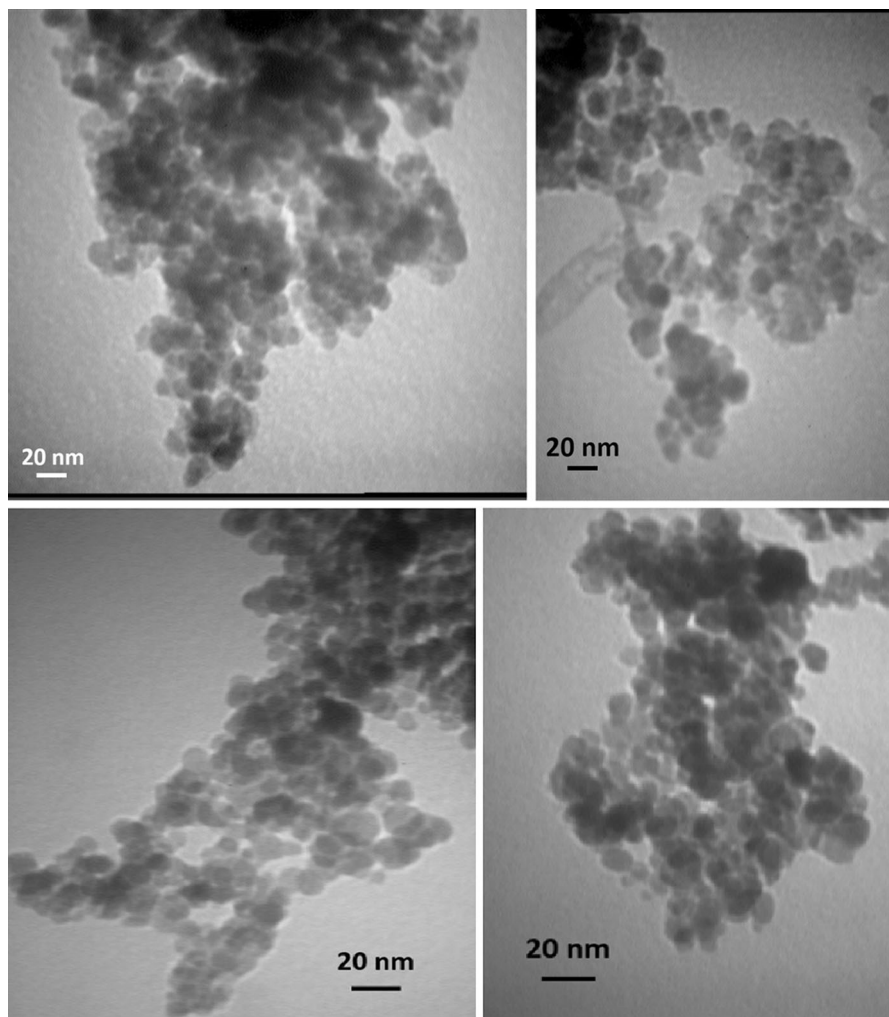


Fig. 2 TEM images of DSA@MNPs

DSA@MNPs, in which the presence of SO_3H moiety is confirmed by $998\text{--}1220\text{ cm}^{-1}$ bands in the FT-IR spectrum, overlapped by C–H stretching vibration. All of those bands reveal that the surface of the Fe_3O_4 nanoparticles was successfully modified with dopamine sulfonic acid.

Functionalization of the Fe_3O_4 nanoparticles with dopamine sulfamic acid can be inferred from the TGA results. Thermogravimetric analysis (TGA) curves of Fe_3O_4 MNPs, MNPs–dopamine, and DSA@MNPs are outlined in Fig. 5. The TGA curves present different mass loss ranges. MNPs–dopamine presents two weight losses. The weight loss in the first step, between 35 and 150°C , can be attributed to removal of surface water and surface hydroxyl groups. The second step of weight loss, between 450 and 680°C , is due to loss of organic groups. The TGA curve for

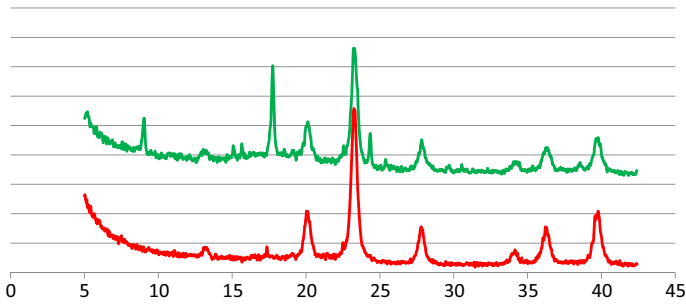


Fig. 3 XRD patterns of DSA@MNPs (green line) and Fe_3O_4 (red line). (Color figure online)

Fig. 4 FT-IR spectra of
a magnetic Fe_3O_4 nanoparticles,
b MNPs–dopamine, and
c DSA@MNPs

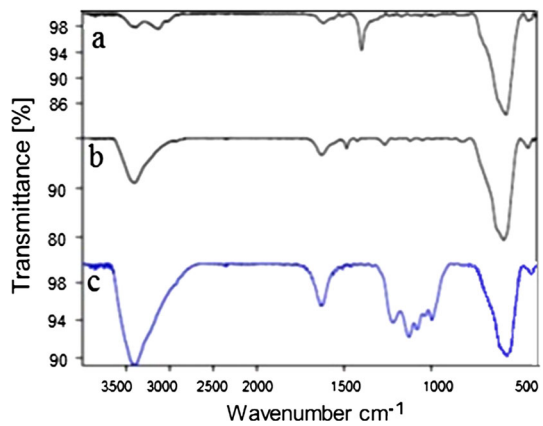
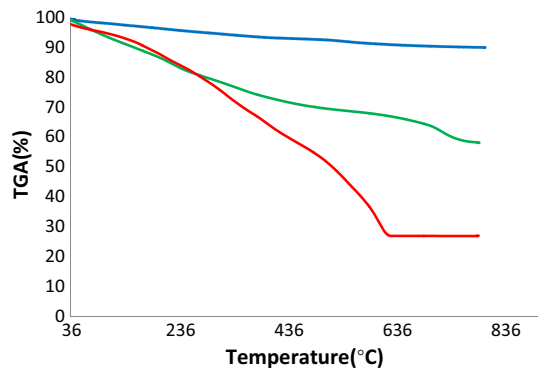


Fig. 5 TGA diagrams of Fe_3O_4 MNPs (blue line), MNPs–dopamine (green line), and DSA@MNPs (red line). (Color figure online)



the DSA@MNPs exhibits three weight loss steps. The first region shows mass loss of about 7.2 %, attributable to removal of physically adsorbed solvent and surface hydroxyl groups. The second weight loss is concentrated at temperature around 250 °C, being due to decomposition of sulfamic acid and formation of sulfur

dioxide. The third weight loss occurs near 500 °C, corresponding to decomposition of organic groups [27].

The thermal stability of the DSA@MNPs was also determined, since synthesis of many organic compounds is usually carried out at high temperature. As shown in Fig. 5, this catalyst was stable even at 220 °C.

To determine the acid amount on the surface, the prepared catalyst (10 mg) was added to aqueous NaCl solution (1 mol/L, 10 mL) with initial pH of 7.9. The mixture was stirred for 0.5 h, after which the pH of the solution had decreased to 4.1, indicating ion exchange between sulfamic acid protons and sodium ions; this is equal to a loading of 0.7 mmol/g of sulfuric acid group. This result was confirmed by back titration of the catalyst.

Catalytic studies

After characterization of the prepared nanocatalyst, in the present work we were also interested in using this compound as an active and stable, magnetically separable nanocatalyst for oxidation of sulfides and oxidative coupling of thiols (Scheme 2).

Oxidation of sulfides to sulfoxides

To determine the best reaction medium, different parameters were investigated for oxidation of dibenzyl sulfide as model reaction, including use of different molar ratios of H₂O₂, amounts of catalyst, and various solvents (Table 1).

Initially, the amount of catalyst was optimized; it was observed that the best results were obtained with 0.02 g catalyst (Table 1, entry 3). Also, these experiments showed that oxidation reaction did not occur in the absence of the catalyst (Table 1, entry 7).

Subsequently, the influence of different solvents was examined (Table 1, entries 1–3). Among the solvents examined, the highest yield was achieved when using ethanol (Table 1, entry 3).

Also, the amount of H₂O₂ in oxidation of tetrahydrothiophene was optimized (Table 2). We found that the reaction did not occur in the absence of H₂O₂ (Table 2, entry 1). Meanwhile, the best results were observed when using 0.5 mL H₂O₂ (Table 2, entry 4).

To determine the role played by iron (Fe) or Fe₃O₄ MNPs and MNPs–dopamine during the reactions, oxidation of tetrahydrothiophene was examined in the presence

Scheme 2 DSA@MNP-catalyzed oxidation of sulfides to sulfoxides and oxidative coupling of thiols into disulfides using H₂O₂

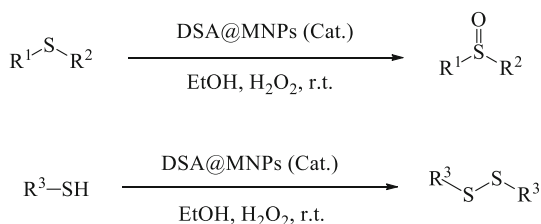


Table 1 Optimization of oxidation of dibenzyl sulfide using dopamine sulfamic acid-functionalized magnetic Fe₃O₄ nanoparticles under various conditions

Entry	Solvent	Catalyst (mg)	Time (min)	Yield (%) ^a
1	Acetone	20	4 h	88
2	<i>n</i> -Hexane	20	24 h	NR
3	EtOH	20	60	98
4	EtOH	15	60	75
5	EtOH	10	60	65
6	EtOH	5	60	53
7	EtOH	–	24 h	–

The reactions were carried out with 1 mmol dibenzyl sulfide, H₂O₂ (0.5 mL), and 10 mL ethanol as solvent at room temperature

^a Isolated yield

Table 2 Oxidation of tetrahydrothiophene in presence of DSA@MNPs in different amounts of H₂O₂ at room temperature

Entry	H ₂ O ₂ (mL)	Time (min)	Yield (%) ^a
1	–	20	– ^b
2	0.3	20	45 ^c
3	0.4	20	65 ^c
4	0.5	20	92
5	0.6	15	94

^a Isolated yield

^b Reaction proceeds in absence of H₂O₂

^c Isolated yield obtained by plate chromatography

Table 3 Effect of Fe₃O₄ MNPs and MNPs–dopamine in comparison with DSA@MNPs in oxidation of tetrahydrothiophene as model compound under optimized conditions

Entry	Substrate	Catalyst	Yield (%) ^a
1	Tetrahydrothiophene	–	Trace ^b
2	Tetrahydrothiophene	Fe ₃ O ₄ MNPs	36 ^c
3	Tetrahydrothiophene	MNPs–dopamine	18 ^c
4	Tetrahydrothiophene	DSA@MNPs	92

^a Isolated yield after 20 min

^b Reaction proceeds in absence of catalyst

^c Isolated yield obtained by plate chromatography

of DSA@MNPs compared with Fe₃O₄ alone and MNPs–dopamine. The results of this comparison are presented in Table 3, revealing that the products were obtained in 36 and 18 % yield in the presence of Fe₃O₄ MNPs and MNPs–dopamine, respectively. These results show that Fe₃O₄ acted as catalyst support and did not

play any role in the oxidation reaction. Also, these results show that Fe ion did not leach during the reaction process.

Oxidative coupling of thiols to disulfides

The next part of the study focused on the utility of this catalyst for oxidative coupling of thiols into their corresponding disulfides. In this reaction, 2-mercaptobenzothiazole was selected as model substrate.

The influence of reaction parameters such as solvents and catalyst amount was tested (Table 4). Among the solvents investigated, ethanol was the best choice due to the high yield and selectivity. To investigate the effect of catalyst amount on the outcome of reaction, the reaction was carried out with different amounts of catalyst; the results are presented in Table 4 (entries 6–10). The best result was obtained with 0.004 g catalyst (Table 4, entry 6).

The generality of this approach was demonstrated by facile oxidation of various sulfides, as presented in Table 5, the sulfoxides being obtained in high yields. As shown in Table 5, a variety of sulfides were successfully employed to prepare the corresponding sulfoxides. The experimental procedure is very simple. Also, various thiols with various functional groups were coupled in the presence of DSA@MNPs under optimized conditions, obtaining the corresponding disulfide compounds in good to excellent yield (Table 5).

A possible mechanistic path for the oxidation of sulfides is shown in Scheme 3. One explanation for this transformation is in situ formation of peroxyacid using the reaction of DSA@MNPs with H_2O_2 , followed by oxygen transfer to the organic substrate (Scheme 3a). Another explanation is that DSA@MNPs act as protic acid, which polarizes the O–O bond in hydrogen peroxide to produce the reactive oxygen transfer agent (Scheme 3b).

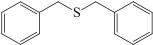
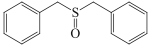
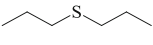
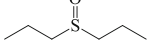
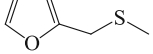
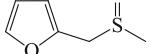
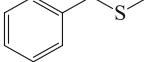
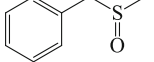
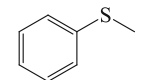
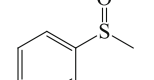
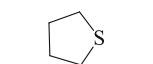
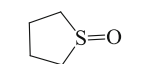
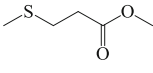
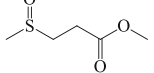
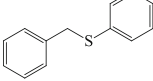
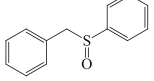
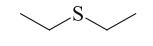
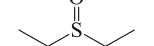
Table 4 Optimization of oxidative coupling of 2-mercaptobenzothiazole using dopamine sulfamic acid-functionalized magnetic Fe_3O_4 nanoparticles under various conditions

Entry	Solvent	Catalyst (mg)	Time (min)	Yield (%) ^a
1	EtOH	4	45	98
2	Acetone	4	240	97
3	<i>n</i> -Hexane	4	44	91
4	Dichloromethane	4	48	98
5	Ethyl acetate	4	30	90
6	EtOH	4	45	98
7	EtOH	3	45	80
8	EtOH	2	45	75
9	EtOH	1	45	42
10	EtOH	–	45	Trace

Reactions carried out with 1 mmol 2-mercaptobenzothiazole, H_2O_2 (0.5 mL), and 10 mL ethanol as solvent at room temperature

^a Isolated yield

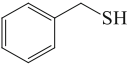
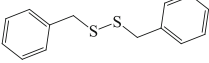
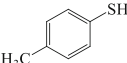
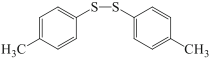
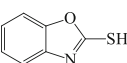
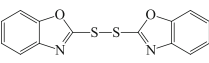
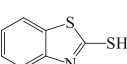
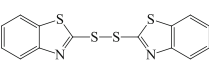
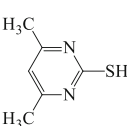
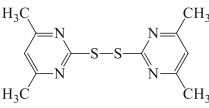

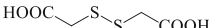

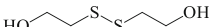
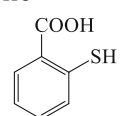
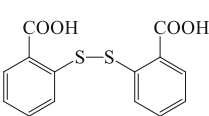
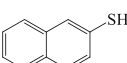
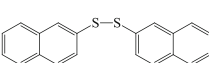
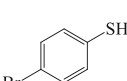
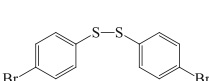
Table 5 Oxidation of sulfides to sulfoxides in presence of DSA@MNPs

$\text{R}^1\text{--S--R}^2 \xrightarrow[\text{EtOH, H}_2\text{O}_2 \text{ (0.5 mL), r.t.}]{\text{DSA@MNPs (0.02 g)}} \text{R}^1\text{--}\overset{\text{O}}{\underset{\text{O}}{\text{S}}}\text{--R}^2$						
Entry	Substrate	Product	Catalyst (g)	Time (h)	Yield (%) ^a	M.p (°C) [Refs.]
1			0.02	1	97	138 [28]
2			0.02	15min	85	Oil [29]
3			0.02	45 min	95	Brown oil [28]
4			0.02	55min	95	Oil [30]
5			0.02	6	98	32 [29]
6			0.02	20 min	92	Oil [31]
7			0.02	40 min	95	Oil [29]
8			0.02	5	97	114–116 [32]
9	$\text{C}_{12}\text{H}_{25}\text{--S--C}_{12}\text{H}_{25}$	$\text{C}_{12}\text{H}_{25}\text{--}\overset{\text{O}}{\underset{\text{O}}{\text{S}}}\text{--C}_{12}\text{H}_{25}$	0.02	5min	95	85–89 [28]
10			0.02	20min	70	103–105 [28]

^a Isolated yield

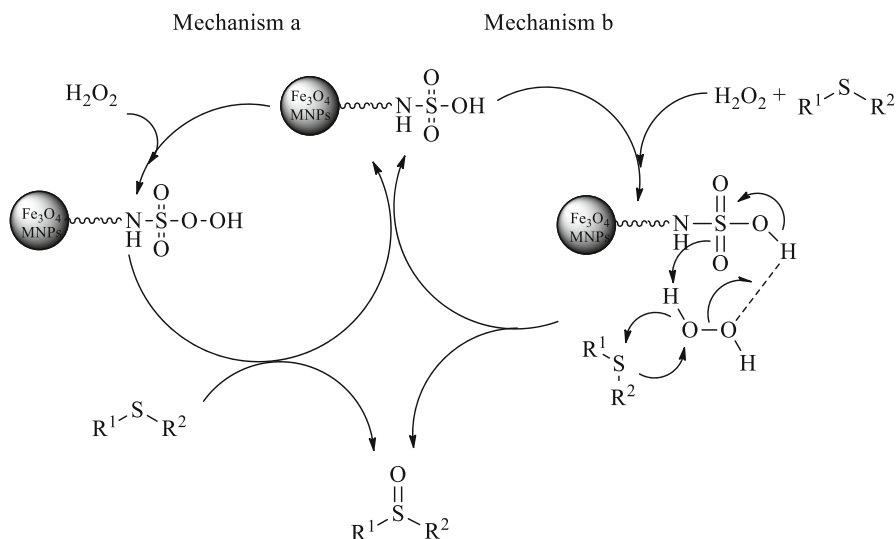
The reusability of catalysts is one of their most important advantages, making them useful for commercial applications. We found that the DSA@MNPs could be rapidly recovered and demonstrated remarkably excellent recyclability. To investigate this issue, the recyclability of this catalyst was examined in oxidation of dibenzyl sulfide and 2-mercaptobenzothiazole. After completion of the reaction, the

Table 6 Oxidative coupling of thiols into disulfides using H₂O₂ in presence of DSA@MNPs

$\text{R}^3\text{-SH} \xrightarrow[\text{EtOH, H}_2\text{O}_2 \text{ (0.5 mL), r.t.}]{\text{DSA@MNPs (0.004 g)}} \text{R}^3\text{-S-S-R}^3$					
Entry	Substrate	Product	Time (min)	Yield (%) ^a	M.p (°C) [Refs.]
1			60	90	69–70 [33]
2			15	97	38–40 [31]
3			90	70	94–96 [28]
4			47	96	174–175 [31]
5			200	70	165–167 [34]
6			90	80	Oil [29]
7			22	81	Oil [31]
8			120	95	274–281 [29]
9			120	90	134–136 [31]
10			180	97	89–90 [29]

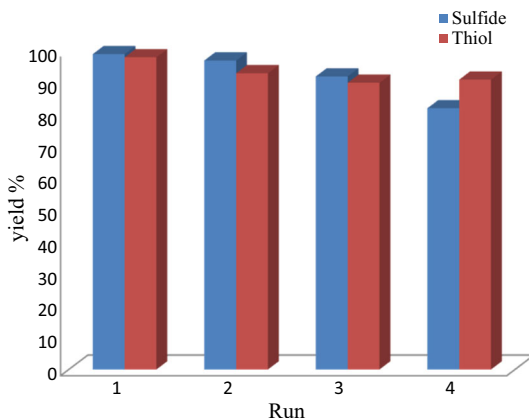
^a Isolated yield

catalyst was separated using an external magnet. The remaining catalyst was washed with ethanol to remove residual product and dried in a hot air oven at 100 °C for 2 h. Then, fresh substrate was added to the remaining catalyst without any activation and employed for the next reaction. As shown in Fig. 6, the catalyst could be recycled in up to four runs without significant loss of catalytic activity.



Scheme 3 Proposed mechanism for oxidation of sulfides in presence of DSA@MNPs as catalyst

Fig. 6 Reusability of DSA@MNPs in oxidation of sulfide (dibenzyl sulfide) and 2-mercaptobenzothiazole



Conclusions

We synthesized novel and recyclable DSA@MNPs and examined their catalytic activity for synthesis of sulfoxide and disulfide derivatives. This active catalyst is thermally stable, inexpensive, and easy to prepare. The advantages of this procedure are use of commercially available, ecofriendly, cheap, and chemically stable oxidant, mild reaction conditions, and operational simplicity. Product separation and catalyst recycling are easier and simpler with the assistance of an external magnet.

Acknowledgments Financial support for this work by the research affairs of Ilam University, Ilam, Iran is gratefully acknowledged.

References

1. O. Salata, J. Nanobiotechnol. **1**, 2 (2004)
2. H. Li, Ch. Xu, N. Srivastava, K. Banerjee, IEEE Trans. Electron. Dev. **1799**, 56 (2009)
3. A. Ghorbani-Choghamarani, F. Nikpour, F. Ghorbani, F. Havasi, RSC Adv. **33212**, 5 (2015)
4. Z.J. Wang, S. Ghasimi, K. Landfester, K.A.I. Zhang, Chem. Mater. **1921**, 27 (2015)
5. H. Veisi, J. Gholami, H. Ueda, P. Mohammadi, M. Noroozi, J. Mol. Catal. A Chem. **216**, 396 (2015)
6. J. Safari, Z. Zarnegar, Ultrason. Sonochem. **740**, 20 (2013)
7. P. Tartaj, M.d.P. Morales, S. Veintemillas-Verdaguer, T. Gonzalez-Carreno, C.J. Serna, J. Phys. D Appl. Phys. **182**, 36 (2003)
8. X. Zhang, M. Lin, X. Lin, C. Zhang, H. Wei, H. Zhang, B. Yang, A.C.S. Appl. Mater. Interfaces **450**, 6 (2014)
9. H. Yang, D. Shi, S.F. Ji, D.N. Zhang, X.F. Liu, Chin. Chem. Lett. **1265**, 25 (2014)
10. W. Li, H. Cheng, Solid State Sci. **750**, 9 (2007)
11. I.V. Kozhevnikov, Appl. Catal. A Gen. **3**, 256 (2003)
12. C.H. Springsteen, L.L. Johnston, R.L. LaDuca, Solid State Sci. **804**, 9 (2007)
13. B. Ren, M. Fan, J. Wang, X. Jing, Solid State Sci. **1594**, 13 (2011)
14. P. Sharma, A.P. Singh, Catal. Sci. Technol. **2978**, 4 (2014)
15. S.S. Soni, D.A. Kotadia, Catal. Sci. Technol. **510**, 4 (2014)
16. M.M. Heravi, S. Sadjadi, J. Iran. Chem. Soc. **1**, 6 (2009)
17. M. Melchionna, S. Marchesan, M. Prato, P. Fornasiero, Catal. Sci. Technol. **3859**, 5 (2015)
18. P. Nehra, B. Khungar, K. Pericherla, S.C. Sivasubramanian, A. Kumar, Green Chem. **4266**, 16 (2014)
19. P.M. Uberman, L.A. Perez, S.E. Martin, G.I. Lacconi, RSC Adv. **12330**, 4 (2014)
20. A. Rostami, B. Tahmasbi, A. Yari, Bull. Korean Chem. Soc. **1521**, 34 (2013)
21. M. Hajjami, B. Tahmasbi, RSC Adv. **59194**, 5 (2015)
22. R. Hekmatshoar, S. Sajadi, M.M. Heravi, F.F. Bamoharram, Molecules **2223**, 12 (2007)
23. J.D. Thomas, T.R. Burke Jr, Tetrahedron Lett. **4316**, 52 (2011)
24. C. Feng, L. Huang, Z. Guo, H. Liu, Electrochem. Commun. **119**, 9 (2007)
25. A. Ghorbani-Choghamarani, B. Ghasemi, Z. Safari, G. Azadi, Catal. Commun. **70**, 60 (2015)
26. A. Ghorbani-Choghamarani, M. Norouzi, J. Mol. Catal. A Chem. **172**, 395 (2014)
27. S. Sobhani, Z. Pakdin Parizi, N. Razavi, Appl. Catal. A Gen. **162**, 409–410 (2011)
28. M. Nikoorazm, A. Ghorbani-Choghamarani, N. Noori, Appl. Organometal. Chem. **328**, 29 (2015)
29. A. Ghorbani-Choghamarani, Z. Darvishnejad, B. Tahmasbi, Inorg. Chim. Acta **223**, 435 (2015)
30. C. Yang, Q. Jin, H. Zhang, J. Liao, J. Zhu, B. Yu, J. Deng, Green Chem. **1401**, 11 (2009)
31. A. Ghorbani-Choghamarani, B. Tahmasbi, F. Arghand, S. Faryadi, RSC Adv. **92174**, 5 (2015)
32. D.Y. Dai, L. Wang, Q. Chen, M.Y. He, J. Chem. Res. **183**, 38 (2014)
33. B. Karami, M. Montazerzohori, M.H. Habibi, Molecules **1358**, 10 (2005)
34. A. Ghorbani-Choghamarani, G. Azadi, B. Tahmasbi, M. Hadizadeh-Hafshejani, Z. Abdi, Phosphorus Sulfur Silicon Relat. Elem. **433**, 189 (2014)